Degradation patterns of silicone-based dielectric elastomers in electrical fields

Yu, Liyun; Madsen, Frederikke Bahrt; Skov, Anne Ladegaard

Published in:
International Journal of Smart and Nano Materials

Link to article, DOI:
10.1080/19475411.2017.1376358

Publication date:
2018

Document Version
Publisher's PDF, also known as Version of record

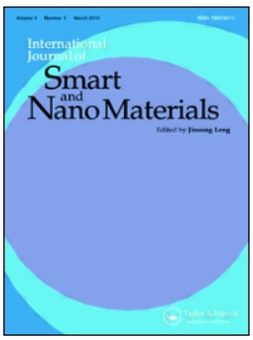

International Journal of Smart and Nano Materials

ISSN: 1947-5411 (Print) 1947-542X (Online) Journal homepage: http://www.tandfonline.com/loi/tsnm20

Degradation patterns of silicone-based dielectric elastomers in electrical fields

Liyun Yu, Frederikke B. Madsen & Anne L. Skov

To cite this article: Liyun Yu, Frederikke B. Madsen & Anne L. Skov (2018) Degradation patterns of silicone-based dielectric elastomers in electrical fields, International Journal of Smart and Nano Materials, 9:4, 217-232, DOI: 10.1080/19475411.2017.1376358

To link to this article: https://doi.org/10.1080/19475411.2017.1376358

Published online: 08 Sep 2017.

INTERNATIONAL JOURNAL OF SMART AND NANO MATERIALS
2018, VOL. 9, NO. 4, 217–232
https://doi.org/10.1080/19475411.2017.1376358

Taylor & Francis
Taylor & Francis Group

ARTICLE

Degradation patterns of silicone-based dielectric elastomers in electrical fields

Liyun Yu, Frederikke B. Madsen and Anne L. Skov

Danish Polymer Centre, Department of Chemical and Biochemical Engineering, Technical University of Denmark, Kgs. Lyngby, Denmark

ABSTRACT

Silicone elastomers have been heavily investigated as candidates for the flexible insulator material in dielectric elastomer transducers and are as such almost ideal candidates because of their inherent softness and compliance. However, silicone elastomers suffer from low dielectric permittivity. This shortcoming has been attempted optimized through different approaches during recent years. Material optimization with the sole purpose of increasing the dielectric permittivity may lead to the introduction of problematic phenomena such as premature electrical breakdown due to high leakage currents of the thin elastomer film. Within this work, electrical breakdown phenomena of various types of permittivity-enhanced silicone elastomers are investigated. Results showed that different types of polymer backbone chemistries lead to differences in electrical breakdown patterns, which were revealed through SEM imaging. This may pave the way towards a better understanding of electrical breakdown mechanisms of dielectric elastomers and potentially lead to materials with increased electrical breakdown strengths.

ARTICLE HISTORY
Received 3 July 2017
Accepted 3 September 2017

KEYWORDS
Silicone elastomers; dielectric; electrical breakdown; voltage stabilization; characterization

1. Introduction

Silicone elastomers are gaining more and more attention for dielectric elastomer applications, mainly due to their inherent reliability which arises from the covalently crosslinked silicone polymer chains. This stands in contrast to the commonly used acrylic adhesive by 3M, namely VHB. VHB has proven to be an excellent material to showcase the possibilities of dielectric elastomers, for example through extreme extensibilities [1,2], but VHB does not possess the required reliability to become a viable, commercial dielectric elastomer transducer material [3,4]. Usually, VHB loses its performance after 100–1000 actuation cycles at large strains, and this lifetime is far from the 10–100 million cycles that is desired for most transducers [5]. Silicone elastomers, conversely, suffer from low dielectric permittivity ($\varepsilon_r = \sim 3$) compared to acrylics ($\varepsilon_r = \sim 5$) and polyurethane-based ($\varepsilon_r = > 5$) elastomers and will thus usually result in a lower actuation response at a given voltage when used as a dielectric elastomer actuator [6]. For some applications, the achievable strain from unmodified silicone elastomers is sufficient such as lenses [7] and valves [8] but for example for wave energy harvesting [9] larger strains will also lead to larger energy generation and thus increased strains are desired. Numerous

CONTACT Anne L. Skov al@kt.dtu.dk Polymer Centre, Department of Chemical and Biochemical Engineering, Technical University of Denmark, Søltofts Plads Building 227 Room 122, Kgs. Lyngby 2800, Denmark

approaches to increase dielectric permittivity of silicone elastomers exist, which include mixing in metal oxides [10–12] or high permittivity liquids [13], covalent grafting of dipoles [14–16] and the use of functional copolymers [17,18]. All methods introduce complex changes in mechanical and electrical properties such that many elastomers with increased permittivity either suffer from increased stiffness, increased leakage currents or decreased electrical breakdown strengths. For more details on the effects of specific methods see the recent review on silicone dielectric elastomer transducers by Madsen et al [5]. Most methods for dielectric permittivity enhancement lead to a reduction in the electrical breakdown strength of the resulting elastomer. Therefore these elastomers will need to be operated at a lower voltage for reliability. This is highly unfavorable, but currently no universal method to increase the electrical breakdown strength of dielectric elastomers exists since the electrical breakdown processes are not fully understood. This circumstance is complicated further by the interplay between electrical and mechanical processes, which may lead to electro-mechanical breakdown processes, usually denoted electro-mechanical instability (EMI) [19–22]. Thus, no guideline on how to formulate soft dielectric elastomers with high electrical breakdown strength exists apart from the generic guidelines on what to avoid such as avoiding percolation of added fillers, which potentially leads to the introduction of conductive paths [23,24]. One approach to increase the electrical breakdown strength is, however, to increase the Young's modulus of the elastomer. This can be done, for example, by adding highly reinforcing, non-conductive metal oxide particles. Nevertheless this method usually causes a significant decrease in the actuation performance at a given voltage due to the increased stiffness of the resulting elastomer.

So-called voltage stabilization of high voltage cable insulation materials has been heavily investigated with the main focus being on thermoplastic or lightly crosslinked polyethylene (PE). The principle relies on the addition to the PE matrix of low-molecular weight compounds such as aromatic substances which then trap electrical charges [25,26]. This requires that the aromatic substances absorb strongly at the energy levels of the labile electrons in the PE material. Thereby avalanche breakdown is avoided or inhibited to some extent. This method is versatile for PE since the required quantities of voltage stabilizers are minute (usually significantly less than 1%) and they can be blended into the polymer matrix with little – if any – phase separation. The attained increases in electrical breakdown strengths are significant – by the inclusion of diversified aromatic substances optimized for a given PE insulator matrix the electrical breakdown strengths have been improved by almost 50% [25,27,28]. This concept should, in theory, be relatively easily transferred to silicone elastomers. However, such – usually aromatic – substances are not miscible in the silicone matrix even in minute concentrations, and thus grafting of the additives at a molecular level is required in order to obtain reliable and reproducible elastomer films. Most silicone elastomer formulations with non-grafted low-molecular weight aromatic substances (i.e. additives) cause an easy detectable macroscopic phase separation with clear aromatic regions leading to local loss of insulating properties. Therefore, voltage stabilization of silicone elastomers becomes a complex task because it is crucial that the elastomer remains insulating and without conductive zones that could lead to build up of space charge [29]. This means, that synthetic approaches to incorporation of additives into the silicone polymer backbone are required and that the final polymer structure must be tailored in such a way that the microscopic phase separation favors voltage stabilization [18] rather than electrical conduction. This renders the design of the silicone elastomer system rather complex.

Recent studies have shown that the use of for example simple dipolar moieties in small amounts can increase the electrical breakdown strength. Such studies include synthetic incorporation of aromatic compounds [18] and chloropropyl groups [30,31] in the silicone polymer backbone. In this study we investigate the electrical breakdown patterns of two chloropropyl-functionalized silicone elastomers as prepared in Madsen et al [30] which break down electrically in rather different ways and we compare them to a silicone-based reference. The chloropropyl-functionalized elastomers are interesting candidates for dielectric elastomer transducers since their overall properties provide great figures of merit [5]. This is mainly due to combination of low Young's modulus, and relatively high dielectric permittivity and electrical breakdown strength, but also due to very low dielectric losses. Thermogravimetric analysis (TGA) and scanning electron microscopy (SEM) are used to evaluate the elastomers before and after electrical breakdown. Furthermore, the TGA potentially provides a basis for evaluation of the energies of chemical degradation (i.e. bond cleavage) involved in the electrical breakdown process.

2. Experimental section

2.1. *Materials*

Vinyl-terminated PDMS, DMS-V31 ($\bar{M}_w \approx 28{,}000$ g mol^{-1}), and a hydride-functional cross-linker, HMS-301, were acquired from Gelest Inc. The platinum cyclovinylmethyl siloxane complex catalyst (511) was purchased from Hanse Chemie, while silicon dioxide amorphous hexamethyldisilazane-treated particles (SIS6962.0) were purchased from Fluorochem. The inhibitor Pt88 was acquired from Wacker Chemie AG, and all other chemicals were acquired from Sigma-Aldrich and used as received, unless otherwise stated.

Two types of copolymers (Co-1 and Co-2) with two different spacer lengths between the chloropropyl-groups were synthesized according to previous work [30].

2.2. *Film preparation*

Co-1, Co-2, or DMS-V31, respectively, and an 8-functional cross-linker HMS-301 were mixed with treated silica particles (25 wt%) and inhibitor (1 wt%, Pt88) and then mixed on a FlackTek Inc. DAC 150.1 FVZ-K SpeedMixer™. The catalyst (511) (1.5 ppm) was added thereafter and the mixture was speed-mixed once more. The uniform mixtures thus made were coated on a glass substrate using a film applicator (3540 bird, Elcometer, Germany) with 150 µm blade. Films were fully cured in the oven for 1 hour at 115°C.

2.3. *Electrical breakdown strength determination*

Electrical breakdown tests were performed on an in-house-built device based on international standards (IEC 60,243–1 (1998) and IEC 60,243–2 (2001)), while film thicknesses were measured through the microscopy of cross-sectional cuts, and the distance between the spherical electrodes was set accordingly with a micrometer stage and gauge. An indent of less than 5% of sample thickness was added, to ensure that the spheres were in contact with the sample. The polymer film was slid between the two spherical electrodes (diameter of 20 mm), and the breakdown was measured at the point of contact by applying a stepwise increasing voltage

(50–100 V step^{-1}) at a rate of 0.5–1 steps s^{-1}. Each sample was subjected to 12 breakdown measurements, and an average of these values was given as the breakdown strength of the sample. The electrical breakdown experimental setup is shown in Figure 1.

2.4. *Young's modulus and tensile strength measurements*

Uniaxial extensional rheology was performed on the series of elastomer films in order to determine the Young's modulus and tensile strength. The stress-strain curves of films were tested at room temperature by ARES-G2 rheometer using the SER2 geometry. A sample of 20 mm length and 6 mm width was placed between two drums and initially separated by a distance of 12.7 mm. The test specimen was elongated uniaxially at steady Hencky strain rate of 0.01 s^{-1} until sample failure at the middle part. Each composition was subjected to four tensile measurements which were then averaged. Young's moduli were obtained from the tangent of the stress-strain curves at 5% strain.

2.5. *Dielectric properties test*

Dielectric relaxation spectroscopy (DRS) was performed on a Novocontrol Alpha-A high-performance frequency analyser (Novocontrol Technologies GmbH & Co) operating in the frequency range 10^{-1}–10^{6} Hz at room temperature and low electrical field (~1 V/mm). The diameter of the tested 0.5–1 mm thick samples was 25 mm.

2.6. *Thermogravimetric analysis (TGA) and differential scanning calorimetry (DSC) measurements*

Thermogravimetric analysis (TGA) was performed on a Discovery TGA from TA Instruments in a nitrogen atmosphere with a heating rate of 10°C min^{-1} from RT to 900°C.

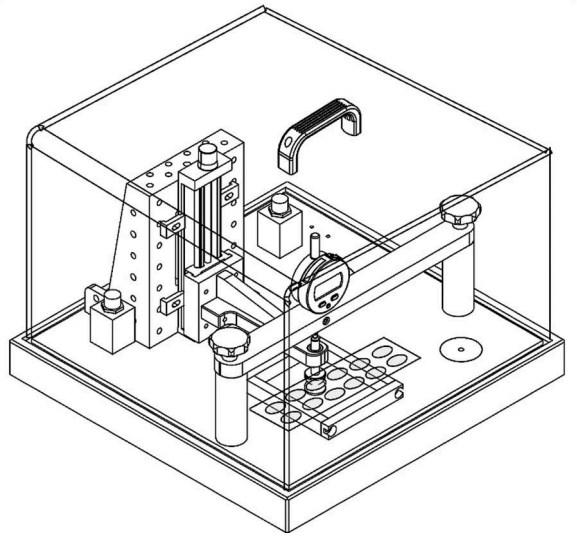

Figure 1. Illustration of electrical breakdown experimental setup.

Differential scanning calorimetry (DSC) measurements were performed on a Discovery DSC from TA Instruments in a nitrogen atmosphere with a heating and cooling rate of 10°C min^{-1} from −150 to 200°C.

2.7. *Scanning electron microscopy (SEM) and microanalysis*

The morphology of the elastomer film breakdown was investigated with an FEI Quanta 200E-SEM environmental scanning electron microscope, equipped with a field emission gun. The surface was visualized in low vacuum, using water vapors as auxiliary gas at a pressure of 150 Pa. A mixture of secondary and back scattered electrons, generated by the sample surface, was detected with the large field detector for an incident electron beam of spot 3 accelerated to 10 keV.

The elemental composition of the elastomer films was determined by energy dispersive X-rays (EDX) with an Oxford Instruments 80 mm^2 X-Max silicon drift detector Mn Kα resolution at 124 eV, also at low vacuum (150 Pa) with a 500 µm pressure limiting aperture X-ray cone. The microanalysis data acquisition and quantification was performed with the Oxford Instruments Aztec program version 3.1.

3. Results and discussion

3.1. *Chemical and mechanical analysis of the prepared elastomers*

Crosslinked chloropropyl-functional silicone elastomers, denoted Co-1 and Co-2, and the reference DMS-V31 were successfully prepared using 8-functional crosslinker, HMS-301, and reinforcing silica particles, giving elastomers with almost identical molecular weight spacing between each crosslink. Details of the prepared elastomers are shown in Table 1. The structure and preparation of the chloropropyl-functional silicone elastomers are illustrated in Scheme 1. The difference between Co-1 and Co-2 is the different spacer lengths between the chloropropyl-groups. Co-1 have 1200 g mol^{-1} dimethylsiloxane spacers between each chloropropyl group, and Co-2 have 580 g mol^{-1} dimethylsiloxane spacers between the functional chloropropyl groups. Co-2, with the shorter spacer, thus contains approximately double the amount of chloropropyl groups than Co-1 prepared with the long spacer (at comparable copolymer lengths) [25]. A summary of the elastomer properties is given in Table 2.

The effect of the chloropropyl-functionalities on the mechanical properties of the elastomers was determined through tensile testing and the results are shown in Table 2. It is evident that the samples possess differences in their elastic properties. The Young's modulus of the reference elastomer is ten times higher than elastomer Co-1 and three times higher than elastomer Co-2. If interpreted entirely from the Young's moduli the electrical breakdown strengths should then follow the trend

Table 1. Details of prepared silicone elastomers.

Name	Molecular weight between crosslinking sites (g mol^{-1})	Concentration of chloropropyl groups (wt%)
DMS-V31	28,000	0
Co-1	29,000	2.0
Co-2	29,000	3.6

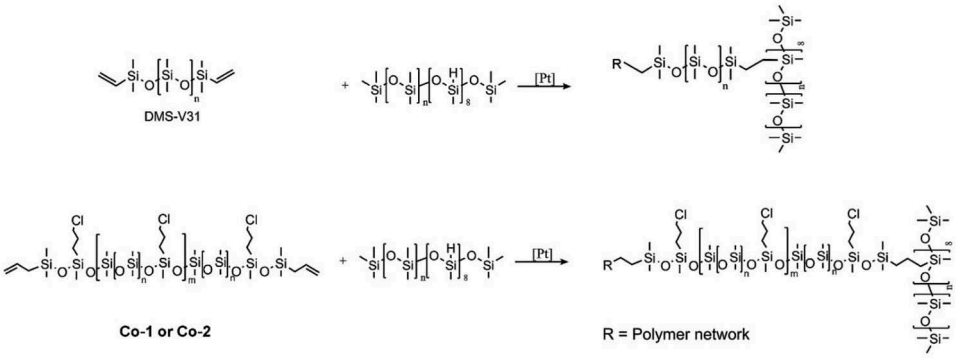

Scheme 1. The structure of chloropropyl-functional silicone elastomers (bottom) and the DMS-V31 reference elastomer (top).

Table 2. Properties of the prepared silicone elastomers. The thermogravimetric data is obtained in nitrogen atmosphere. The mechanical properties are measured at room temperature.

Sample	T_g[a] (°C)	$T_{d3\%}$[b] (°C)	T_{max}[c] (°C)	Residue[d] @900 °C (%)	$E_{breakdown}$ (V μm^{-1})	Y@5% strain (MPa)	Tensile strength (MPa)	Strain at break (%)	ε_r @0.1Hz
DMS-V31	−117.2	414	670	58	82	1.81	6.08	374	3.3
Co-1	−120.4	320	652	51	74	0.15	0.65	429	4.7
Co-2	−116.8	323	665	56	94	0.52	1.27	314	5.1

[a]Glass transition temperature determined by DSC.
[b]Temperature of 3 wt% loss determined by TGA.
[c]Temperature of the maximum degradation rate determined by TGA.
[d]Inorganic residue at 900°C.

$E_{breakdown}$(ref)> $E_{breakdown}$(Co-2) >$E_{breakdown}$(Co-1) since electrical breakdown strength increases with increasing Young's modulus. As seen from the electrical breakdown strength results shown in Table 2 this is apparently not correct and will be discussed in further detail later. With respect to tensile strengths, the reference sample outperforms the two chloropropyl-functional elastomers almost proportionally to the Young's moduli since the elastomers behave more or less as ideal Hookean solids in the entire strain regime. All samples have similar maximum extensions (314–429%). For silicone elastomers the temperature dependency on mechanical properties is weak [32] so no full temperature range characterization has been performed.

3.2. *Electro-mechanical evaluation*

The electromechanical properties of the Co-1 and Co-2 elastomers are evaluated through a comparison with the properties of the commercially available silicone elastomer film from Wacker Chemie AG whose properties resemble that of Elastosil RT625 (likewise from Wacker Chemie AG). The evaluation and comparison is done by normalizing with the electro-mechanical properties of the commercial elastomer film in a comparable thickness. The synthesized reference DMS-V31 is not included in the evaluation since it is solely used as a reference with respect to the thermal and electrical properties.

The figure of merit for actuation is given by [33]:

$$F_{om}(DEA) = \frac{3\varepsilon_r\varepsilon_0 E_{breakdown}^2}{Y} \quad (1)$$

where $E_{breakdown}$ is the electrical field at which electrical breakdown occurs, ε_r is the relative dielectric permittivity, ε_o is the permittivity of free space (8.85×10^{-12} F m^{-1}) and Y is the Young's modulus of the elastomer,

The figure of merit for energy generation is given by [34]:

$$F_{om}(DEG) = \frac{\varepsilon_r\varepsilon_0 E_{breakdown}^2}{2\Phi} \quad (2)$$

where Φ is the energy density function of the investigated elastomer. Due to lack of data for most silicone elastomers it is usually regarded as a constant and is thus ignored in relative comparisons [5].

The properties of Elastosil RT625 for the comparison are regarded as ε_r @0.1Hz = 3, Y@5% strain = 1 MPa and $E_{breakdown}$ = 80 V μm^{-1}[5]. The normalized F_{om}(DEA) of Co-1 and Co-2 elastomers with respect to the commercial reference become 8.9 and 4.5, respectively. In other words, actuation at ultimate conditions of the developed elastomers is 9 and 4.5 times better than the commercial reference elastomer. The normalized F_{om}(DEG) of Co-1 and Co-2 elastomers are 1.3 and 2.3, respectively, i.e. the developed elastomers are interesting to a greater extent from an actuation point of view than for energy generating since only minor improvements in F_{om}(DEG) are achieved. For the figures of merit, the normalized numbers state the improved performance at ultimate conditions, i.e. just before the electrical breakdown of the given insulating film compared to the reference film at its ultimate conditions. Here it is assumed that the dielectric elastomer will always fail electrically before a mechanical rupture takes place, which from Table 2 can be seen as a reasonable assumption since all films survive more than 300% strain in a pure mechanical deformation.

It is evident from the calculated figures of merits that the elastomers with chloropropyl-functional groups show improved dielectric elastomer performance for both actuation and energy generation applications. However, the main improvement was found for actuation due to the low Young's modulus of the elastomers. Usually a low Young's modulus causes low electrical breakdown strength [5,35] but due to the voltage stabilizing effect of the chloropropyl groups the developed elastomers do not follow this trend and thus the materials are from a fundamental point of view interesting to investigate further.

3.3. *Thermal properties and electrical breakdown*

Electrical breakdown may occur through thermal breakdown mechanisms, i.e. heating takes place locally and the heating results in increased conductivity which then again leads to further Joule heating. Thus an accelerating coupling arises since conductivity scales exponentially with temperature. The heating may lead to instantaneous breakdown due to an increased field but may also *a priori* lead to degradation of the elastomer and thus loss of mass, which then subsequently leads to electro-mechanical breakdown due to decreased thickness. When the elastomer starts degrading it may even experience reduced mechanical properties locally in such a way that the elastomer

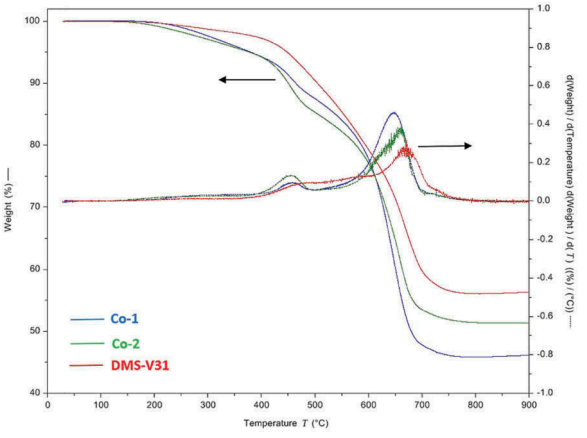

Figure 2. Thermal gravimetrical analysis of chloropropyl-functional silicone elastomers. The analysis was performed in a nitrogen atmosphere with a heating rate of 10°C min^{-1} from room temperature to 900°C.

collapses mechanically. With these scenarios in mind the thermal breakdown patterns are investigated in order to elucidate at which temperatures the elastomers degrade in a nitrogen atmosphere (which is assumed a comparable atmosphere to that of a dielectric elastomer sealed within metallic electrodes).

The thermogravimetric data of the chloropropyl-functional elastomers and the reference DMS-V31 are shown in Figure 2. The thermal degradation temperatures for the samples prepared with chloropropyl-functional copolymers decreases slightly compared to the reference DMS-V31 but remained within the same range. Evidently the synthesized chloropropyl-functional elastomers are very stable with respect to temperature and are not fully degraded before a temperature of around 660 °C is reached, as seen in Table 2. A reduction of $T_{d3\%}$ (the temperature at which 3% by mass is degraded) is observed when the amount of chloropropyl groups is increased indicating that the chloropropyl group – as expected – does not stabilize the silicone elastomer thermally compared to the reference elastomer based solely on PDMS. However, it is unexpected that the Co-1 elastomer is the least thermally stable composition and the Co-2 elastomer resembles the reference elastomer the most with respect to thermal degradation behaviour. A gradual change from the reference over Co-1 to Co-2 was expected due to the increased chloropropyl content. The results are reproducible and the different behaviour between the two chloropropyl-functional elastomers is most likely a result of the spacing between the chloropropyl groups of Co-1 which allows for an easier ring formation of the degradation products, namely cyclic siloxanes [36]. This difference will be discussed later in connection with the electrical breakdown characterization.

3.4. *Breakdown analysis*

Typical breakdown zones in silicone-based elastomers consist of a pinhole with a surrounding region of solidification, both within and on top of the elastomer. This is illustrated in Figure 3. Three different breakdown zones (pinholes and surrounding area)

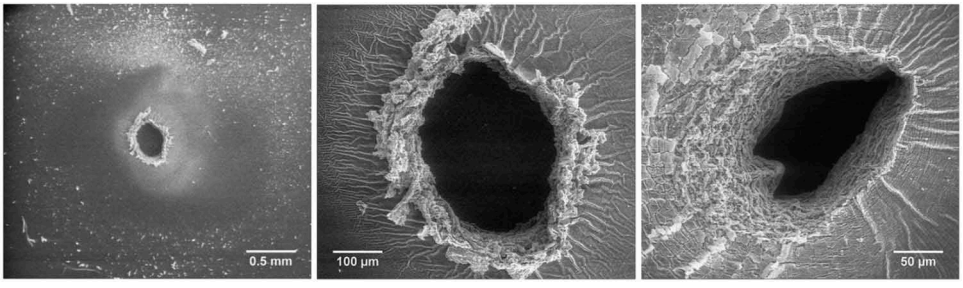

Figure 3. Illustration of common brittle failures after electrical breakdown for the reference DMS-V31. For all three breakdown zones there is a large extent of solidified matter around the pin-hole.

of identical elastomers (reference DMS-V31 sample) are shown. The key observation is that there is a large extent of solidified matter around the pinhole as well as solidified 'threads' spreading from the pinhole outwards. These threads are unfortunate since they lead to stress inhomogeneities, which may potentially lead to tearing of the elastomer film if the breakdown experiment (or actuation) is performed in a non-zero stress configuration. The threads are not solely surface phenomena and span into the bulk of the material. Usually congruent patterns on both back and front side of the film are observed if the elastomer is inserted in the breakdown equipment in an unstretched configuration. If small stretches occur, the top and bottom sides of the film usually look different due to stresses not necessarily in the film area plane. Stretching during mounting is of course attempted avoided in every single experiment but small stresses during the mounting are inevitable. The observed 'threads' may be similar to that of breakdown in solid dielectrics where treeing is a common breakdown mechanism. However, at the current state it is not conclusive whether the threads are a result of the combination of excessive heating and the softness of the material leading to a mechanical phenomenon or if the threads are of electrical nature, i.e. due to charge delocation (or a combination thereof).

For the prepared elastomers varying degree of damage to the material upon electrical breakdown was observed. Two different types of breakdown patterns can be seen for the two chloropropyl-functional elastomers even though their chemical structure is rather similar with the only difference being the concentration of the chloropropyl groups. Examples of such patterns for all three elastomers, Co-1, Co-2 and the reference DMS-V31, are shown in Figure 4. The breakdown zones of the three different elastomers do not look identical but the appearance is rather consistent within one elastomer type. This gives a clear indication that minor changes to the backbone of the silicone elastomer may result in significant changes to electrical breakdown behaviours. The tearing process originating from the breakdown zones is a major challenge in silicone-based dielectric elastomer transducer products since the inherent tear strength of silicone elastomers is usually rather low [37].

The presence of relatively large amounts of chloropropyl groups stabilizes the silicone elastomer electro-mechanically since the Co-2 elastomer has significantly larger electrical breakdown strength than the Co-1 elastomer (Table 2). This effect can partly be attributed to increased stiffness of the elastomer since Co-2 has a significantly larger Young's modulus than the Co-1 elastomer. However, with respect to the reference elastomer, increased

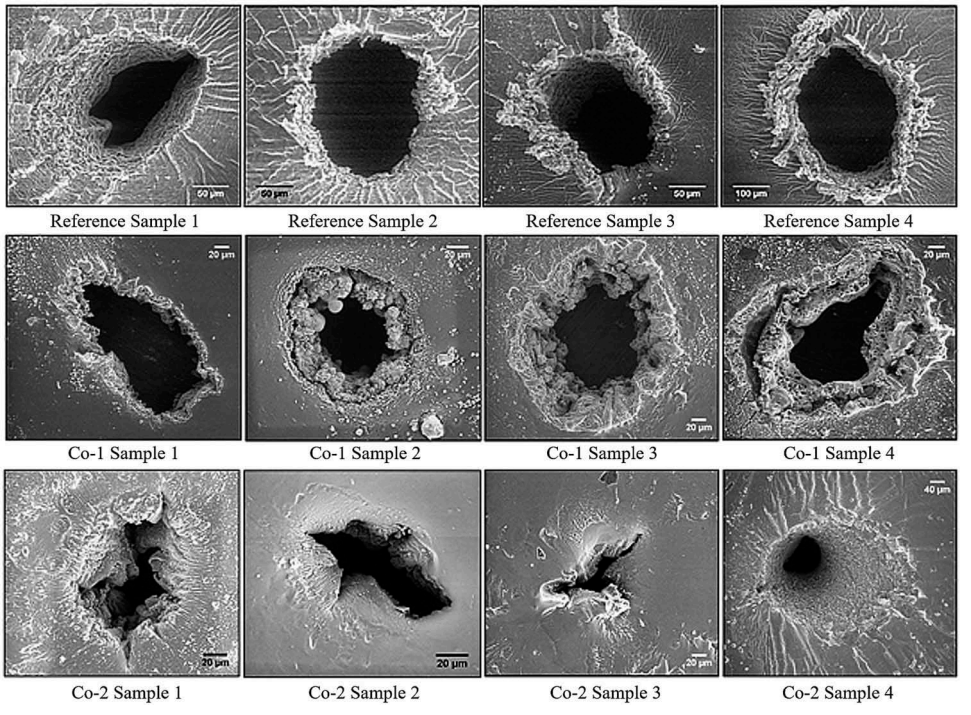

Figure 4. Scanning electron micrographs of breakdown zones for four reference samples (top images), four Co-1 silicone elastomers (middle images), and four Co-2 silicone elastomers (bottom images). The black areas correspond to areas where the elastomer was completely cleared away during breakdown, i.e. pinholes. The white areas are solidified material with high content of silicon. Not all scale bars are identical in order to show the most important features of the specific breakdown zones, which vary dimensionally from narrowest width of around 40 μm to largest width of around 400 μm. $E_{breakdown}$(Reference Sample 1) = 78 V/μm, $E_{breakdown}$(Reference Sample 2) = 81 V/μm, $E_{breakdown}$(Reference Sample 3) = 83 V/μm, $E_{breakdown}$(Reference Sample 4) = 86 V/μm, $E_{breakdown}$(Co-1 Sample 1) = 71 V/μm, $E_{breakdown}$(Co-1 Sample 2) = 74 V/μm, $E_{breakdown}$(Co-1 Sample 3) = 77 V/μm, $E_{breakdown}$(Co-1 Sample 4) = 75 V/μm, $E_{breakdown}$(Co-2 Sample 1) = 95 V/μm, $E_{breakdown}$(Co-2 Sample 2) = 97 V/μm, $E_{breakdown}$(Co-2 Sample 3) = 92 V/μm, and $E_{breakdown}$(Co-2 Sample 4) = 93 V/μm.

stiffness cannot be the explanation for increased breakdown strength of Co-2 since it is softer than the reference. Still the increase in breakdown strength is significant. The Co-2 elastomer possess an average electrical breakdown strength of 20 V μm^{-1} higher than the Co-1 elastomer and break down in what seems to be a more commonly observed pattern, namely through solidification of the elastomer around the pinhole and subsequent partial tearing due to the developed stress gradients around the solidified threads. This gives a clear indication that a certain concentration of chloropropyl groups has a positive effect on the electrical properties, either because the given concentration leads to a better morphology and/or better electrical stabilization. Decoupling the two effects is at current not possible but will be pursued in the future.

As is clearly seen in the SEM images, Co-1 and Co-2 decompose differently during the imposed electrical breakdown. The breakdown of Co-1 is seen to involve substantial boiling and subsequent condensation of volatiles evident in more detail in Figure 5.

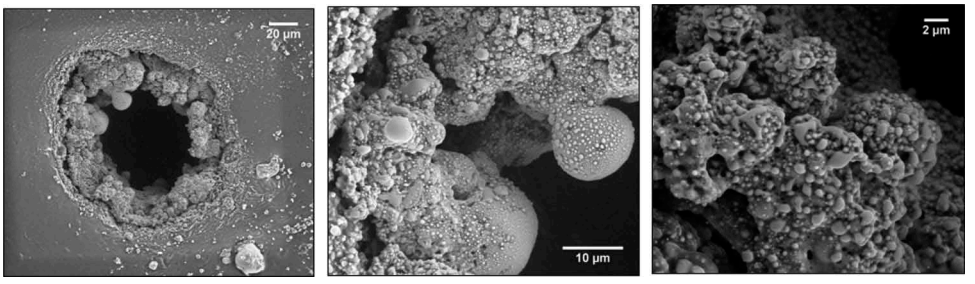

Figure 5. Illustration of the boiling nature of the Co-1 elastomer upon electrical breakdown in different magnifications. Droplets of condensed degradation products are formed on the surface of the breakdown zone. Very little solidification is observed upon the introduced electrical breakdown in this elastomer, and most importantly, there is no solidified thread formation.

In order to get a better idea of the involved breakdown phenomena, SEM/micro-analysis was performed as well. The composition of the solidified zones in the Co-2 elastomer could not be detected due to lack of difference in elemental composition. But very interestingly, as is shown in Figure 6, it is apparent that during the breakdown of Co-1 elastomer silicon-containing substances are burnt off and a chlorine-rich region remains. This could indicate that the siloxane spacer units between the chloropropyl groups are released as cyclics (which are common degradation products of polysiloxanes [38]) during the electrical breakdown process.

For the Co-2 elastomer the elemental composition is comparable throughout the breakdown zone. Interestingly, one would expect HCl to form as a degradation by-product (such as for polyvinyl chloride) but this does not seem to be the case for any of the synthesized chloropropyl-based elastomers (at least it takes place to less extent than the formation of volatile siloxane-based degradation products). The formation of HCl would lead to an auto-degradative process since a highly acidic environment is well

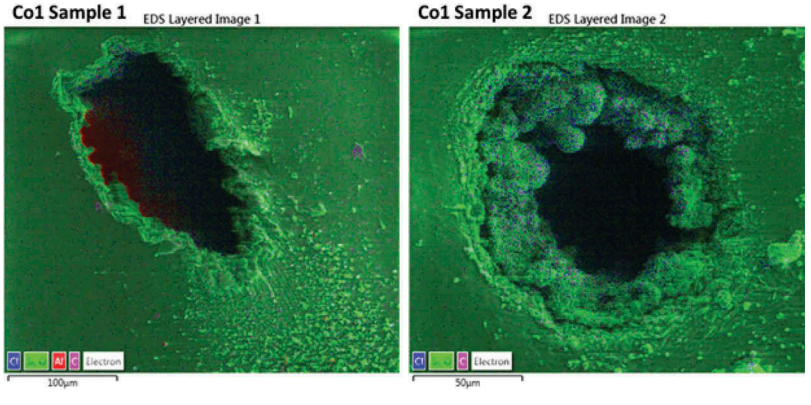

Figure 6. EDS mapping of the breakdown zones for the Co-1 elastomer. The material in vicinity of the pin-hole contains excess of chlorine (blue color), which support the hypothesis that silicon-containing substances have evaporated. Aluminum traces arise from the aluminum stub underneath the pinholes, onto which the elastomer is mounted for the electron microscopy. EDS color legend: Blue: Chlorine, Green: Silicon and Oxygen, Pink: Carbon and Red: Aluminum.

known to cause degradation of silicone polymers [39]. From the thermal gravimetric analysis of the investigated elastomers (shown in Figure 2), it is obvious that in terms of energies involved in the electrical breakdown correspond to the energies from a solely thermal degradation process of more than 500°C.

Another explanation for the variations in the breakdown zones may be the energy dissipated during the electrical breakdown. Since the Co-1 elastomer breaks down at lower electrical fields than the two other elastomers, Co-2 and DMS-V31, there will also most likely be the smallest excessive energy involved. The burnt volumes (determined from the outer dimensions of the breakdown zones, which equal the pinhole volume for the elastomers with no tendency to boiling) and breakdown areas (from top views) have been determined by scanning through breakdown zones by means of SEM. The resulting data is shown in Figure 7 and in Figure 8 tilted SEM images are shown to illustrate how the volume was determined by measuring out distances for various tilting angles.

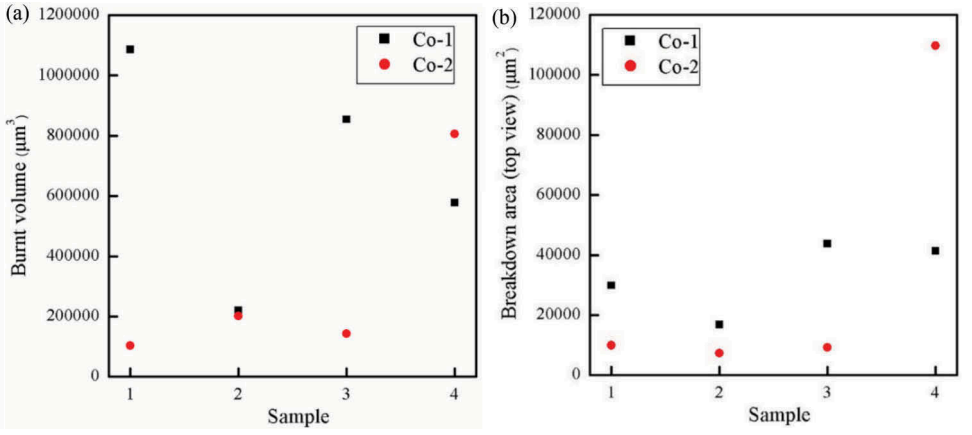

Figure 7. Breakdown zone analysis of Co-1 and Co-2 silicone elastomers for four different samples as shown in Figure 5. The breakdown area is determined from a top view rather than a scan through the elastomer thickness as done for the pinhole volume determination.

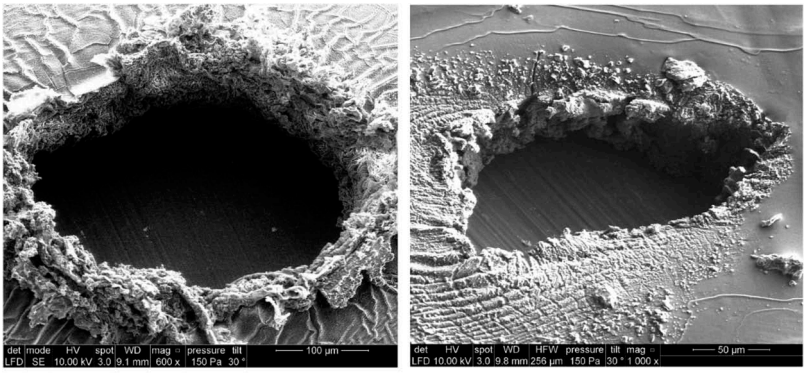

Figure 8. Tilted view of reference sample and Co-1. Scans through the thickness of the film are used to determine the volume of the pinhole.

As can be observed from Figure 7, the average burnt volume for Co-2 elastomer is smaller than for Co-1 elastomer despite the significantly larger electrical field at breakdown. In other words, for the Co-1 elastomer the energy is efficiently transferred to boiling rather than into solidification and subsequent tearing. For the Co-2 elastomer full evaporation is hindered and thus excessive energies are transferred through the elastomer leading to solidification of the silicone part of the elastomer in the traditional way. It means that the two chloropropyl-functional elastomers undergo very different breakdown mechanisms despite the sole difference being the concentration of the chloropropyl groups.

Summing up, the Co-1 elastomer breaks down prematurely in a static electrical breakdown experiment (compared to the two other elastomers) but in contrast the breakdown zones are all without possible tear propagation from solidified threads. This can be explained by electrical energy being consumed in the evaporation process of the volatiles rather than in solidification. However, despite the premature breakdown the Co-1 elastomer may be a better candidate for dielectric elastomer products since the tendency of local (microscopic) electrical breakdown with subsequent macroscopic tearing will be reduced.

Yet another interesting aspect will be to investigate if pre-stretch possibly change the electrical breakdown patterns. In recent work from our group it was proven that the electrical breakdown strength of silicone elastomers strongly improves with pre-stretch [40] even when accounting for the decreased elastomer thickness. This investigation is, however, complicated by the fact that the electrical breakdown of the highly stretched films leads to tearing of the film and thus quantitatively measuring the breakdown zones is difficult.

4. Conclusions

It was shown that chemically very similar silicone elastomers break down electrically in very different ways. These observations emphasize that the modification of the silicone backbone may open up for completely new possibilities for stabilizing the silicone elastomer electrically. In order to tailor the dielectric elastomers, more knowledge is needed but the results of these chloropropyl-functional elastomers pave the first path towards a better understanding of the complex connection between electrical stability and thermal stability and morphology. Minor changes in the polymer backbone structure and chemistry result in changes in electrical breakdown patterns and understanding why is crucial for the design of extraordinarily stable elastomers and thus ultimately reliable dielectric elastomer-based products.

Acknowledgements

The authors wish to express thanks to Ramona Valentina Mateiu (Hempel Foundation Coatings Science and Technology Center, DTU) to help with SEM and EDS investigation.

Disclosure statement

No potential conflict of interest was reported by the authors.

Funding

The Danish Research Council is greatly acknowledged for the funding provided for Frederikke Bahrt Madsen.

References

[1] R. Pelrine, R. Kornbluh, Q. Pei, and J.J.R. Pelrine, *High-speed electrically actuated elastomers with strain greater than 100%*, Science 287 (2000), pp. 836–839. doi:10.1126/science.287.5454.836

[2] X. Zhao and Z. Suo, *Theory of dielectric elastomers capable of giant deformation of actuation*, Phys. Rev. Lett. 104 (2010), pp. 178302. doi:10.1103/PhysRevLett.104.178302

[3] S. Michel, X.Q. Zhang, M. Wissler, C. Löwe, and G. Kovacs, *A comparison between silicone and acrylic elastomers as dielectric materials in electroactive polymer actuators*, Polym. Int. 59 (2010), pp. 391–399. doi:10.1002/pi.2751

[4] S. Rosset, S. Araromi, S. Schlatter, and H. Shea, *Fabrication process of silicone-based dielectric elastomer actuators*, J. Visualized Exp. 2016 (2016), pp. 53423. doi:10.3791/53423

[5] F.B. Madsen, A.E. Daugaard, S. Hvilsted, and A.L. Skov, *The current state of silicone-based dielectric elastomer transducers*, Macromol. Rapid Commun. 37 (2016), pp. 378–413. doi:10.1002/marc.201500576

[6] P. Brochu and Q. Pei, *Advances in dielectric elastomers for actuators and artificial muscles*, Macromol. Rapid Commun. 31 (2010), pp. 10–36. doi:10.1002/marc.200900425

[7] L. Maffli, S. Rosset, M. Ghilardi, F. Carpi, and H. Shea, *Ultrafast all-polymer electrically tunable silicone lenses*, Adv. Funct. Mater. 25 (2015), pp. 1656–1665. doi:10.1002/adfm.201403942

[8] M.A. Unger, H.P. Chou, T. Thorsen, A. Scherer, and S.R. Quake, *Monolithic microfabricated valves and pumps by multilayer soft lithography*, Science 288 (2000), pp. 113–116. doi:10.1126/science.288.5463.113

[9] R.D. Kornbluh, R. Pelrine, H. Prahlad, A. Wong-Foy, B. McCoy, S. Kim, J. Eckerle, and T. Low, *From boots to buoys: Promises and challenges of dielectric elastomer energy harvesting*, SPIE Proc. 7976 (2011), pp. 797605-1–797605-19. doi:10.1117/12.882367

[10] G. Ştiubianu, A. Soroceanu, C.-D. Varganici, C. Tugui, and M. Cazacu, *Dielectric elastomers based on silicones filled with transitional metal complexes*, Compos.Part. B: Eng. 93 (2016), pp. 236–243. doi:10.1016/j.compositesb.2016.03.005

[11] L. Yu and A.L. Skov, *Silicone rubbers for dielectric elastomers with improved dielectric and mechanical properties as a result of substituting silica with titanium dioxide*, Int. J. Smart Nano Mater. 6 (2016), pp. 268–289. doi:10.1080/19475411.2015.1119216

[12] G. Gallone, F. Carpi, D.D. Rossi, G. Levita, and A. Marchetti, *Dielectric constant enhancement in a silicone elastomer filled with lead magnesium niobate-lead titanate*, Mater. Sci. Eng.: C 27 (2007), pp. 110–116. doi:10.1016/j.msec.2006.03.003

[13] P. Mazurek, L. Yu, R. Gerhard, W. Wirges, and A.L. Skov, *Glycerol as high-permittivity liquid filler in dielectric silicone elastomers*, J. Appl. Polym. Sci. 133 (2016), pp. 44153. doi:10.1002/app.44153

[14] F.B. Madsen, L. Yu, A.E. Daugaard, S. Hvilsted, and A.L. Skov, *Silicone elastomers with high dielectric permittivity and high dielectric breakdown strength based on dipolar copolymers*, Polymer 55 (2014), pp. 6212–6219. doi:10.1016/j.polymer.2014.09.056

[15] C. Tugui, S. Vlad, M. Iacob, C.D. Varganici, L. Pricop, and M. Cazacu, *Interpenetrating poly (urethane-urea)-polydimethylsiloxane networks designed as active elements in electromechanical transducers*, Polym. Chem. 7 (2016), pp. 2709–2719. doi:10.1039/C6PY00157B

[16] C. Racles, M. Alexandru, A. Bele, V.E. Musteata, M. Cazacua, and D.M. Opris, *Chemical modification of polysiloxanes with polar pendant groups by co-hydrosilylation*, RSC Adv. 4 (2014), pp. 37620–37628. doi:10.1039/C4RA06955B

[17] A.H.A. Razak, P. Szabo, and A.L. Skov, *Enhancement of dielectric permittivity by incorporating PDMS-PEG multiblock copolymers in silicone elastomers*, RSC Adv. 5 (2015), pp. 53054–53062. doi:10.1039/C5RA09708H

[18] A.H.A. Razak and A.L. Skov, *Silicone elastomers with covalently incorporated aromatic voltage stabilisers*, RSC Adv. 7 (2017), pp. 468–477. doi:10.1039/C6RA25878F

[19] D. Gatti, H. Haus, M. Matysek, B. Frohnapfel, C. Tropea, and H.F. Schlaak, *The dielectric breakdown limit of silicone dielectric elastomer actuators*, Appl. Phys. Lett. 104 (2014), pp. 052905. doi:10.1063/1.4863816

[20] A. Troels, A. Kogler, R. Baumgartner, R. Kaltseis, C. Keplinger, R. Schwoediauer, I. Graz, and S. Bauer, *Stretch dependence of the electrical breakdown strength and dielectric constant of dielectric elastomers*, Smart Mater. Struct. 22 (2013), pp. 104012. doi:10.1088/0964-1726/22/10/104012

[21] X. Zhao, W. Hong, and Z. Suo, *Electromechanical hysteresis and coexistent states in dielectric elastomers*, Phys. Rev. B 76 (2007), pp. 134113. doi:10.1103/PhysRevB.76.134113

[22] X. Zhao and Z. Suo, *Method to analyze electromechanical stability of dielectric elastomers*, Appl. Phys. Lett. 91 (2007), pp. 061921. doi:10.1063/1.2768641

[23] K. Goswami, A.E. Daugaard, and A.L. Skov, *Dielectric properties of ultraviolet cured poly (dimethyl siloxane) sub-percolative composites containing percolative amounts of multi-walled carbon nanotubes*, RSC Adv. 5 (2015), pp. 12792–12799. doi:10.1039/C4RA14637A

[24] B. Kussmaul, S. Risse, G. Kofod, R. Waché, M. Wegener, D.N. McCarthy, H. Krüger, and R. Gerhard, *Enhancement of dielectric permittivity and electromechanical response in silicone elastomers: Molecular grafting of organic dipoles to the macromolecular network*, Adv. Funct. Mater. 21 (2011), pp. 4589–4594. doi:10.1002/adfm.201100884

[25] V. Englund, R. Huuva, S.M. Gubanski, and T. Hjertberg, *High efficiency voltage stabilizers for XLPE cable insulation*, Polym. Degrad. Stab. 94 (2009), pp. 823–833. doi:10.1016/j.polymdegradstab.2009.01.020

[26] A.H.A. Razak, L. Yu, and A.L. Skov, *Voltage-stabilised elastomers with increased relative permittivity and high electrical breakdown strength by means of phase separating binary copolymer blends of silicone elastomers*, RSC Adv. 7 (2017), pp. 17848–17856. doi:10.1039/c7ra02620j

[27] Y. Yamano, *Roles of polycyclic compounds in increasing breakdown strength of LDPE film*, IEEE Trans. Dielectr. Electr. Insul. 13 (2006), pp. 773–781. doi:10.1109/TDEI.2006.1667735

[28] Y. Yamano and H. Endoh, *Increase in breakdown strength of PE film by additives of azocompounds*, IEEE Trans. Dielectr. Electr. Insul. 5 (1998), pp. 270–275. doi:10.1109/94.671957

[29] G.C. Montanari and P.H.F. Morshuis, *Space charge phenomenology in polymeric insulating materials*, IEEE Trans. Dielectr. Electr. Insul. 12 (2005), pp. 754–767. doi:10.1109/TDEI.2005.1511101

[30] F.B. Madsen, L. Yu, A.E. Daugaard, S. Hvilsted, and A.L. Skov, *A new soft dielectric silicone elastomer matrix with high mechanical integrity and low losses*, RSC Adv. 5 (2015), pp. 10254–10259. doi:10.1039/C4RA13511C

[31] F.B. Madsen, L. Yu, P. Mazurek, and A.L. Skov, *A simple method for reducing inevitable dielectric loss in high-permittivity dielectric elastomers*, Smart Mater. Struct 25 (2016), pp. 075018. doi:10.1088/0964-1726/25/7/075018

[32] M. Miwa, A. Takeno, K. Hara, and A. Watanable, *Volume fraction and temperature dependence of mechanical properties of silicone rubber particulate/epoxy blends*, Composites 26 (1995), pp. 371–377. doi:10.1016/S0010-4361(06)80136-9

[33] P. Sommer-Larsen and A.L. Larsen, *Materials for dielectric elastomer actuators*, SPIE Proc. 5385 (2004), pp. 68–77. doi:10.1117/12.539500

[34] T.G. McKay, E. Calius, and I.A. Anderson, *Dielectric constant of 3M VHB: A parameter in dispute*, SPIE Proceeding 7287 (2009), pp. 72870P-1–72870P-10. doi:10.1117/12.815821

[35] F. Carpi, G. Gallone, F. Galantini, and D.D. Rossi, *Silicone-poly(hexylthiophene) blends as elastomers with enhanced electromechanical transduction properties*, Adv. Funct. Mater. 18 (2008), pp. 235–241. doi:10.1002/adfm.200700757

[36] G. Camino, S.M. Lomakin, and M. Lageard, *Thermal polydimethylsiloxane degradation. Part 2. The degradation mechanisms*, Polymer 43 (2002), pp. 2011–2015. doi:10.1016/S0032-3861(01)00785-6.

[37] S. Vudayagiri, M.D. Junker, and A.L. Skov, *Factors affecting the surface and release properties of thin polydimethylsiloxane films*, Polymer J. 45 (2013), pp. 871–878. doi:10.1038/pj.2012.227
[38] M. Narisawa, *Silicone resin applications for ceramic precursors and composites*, Materials 3 (2010), pp. 3518–3536. doi:10.3390/ma3063518
[39] J. Feng, Q. Zhang, Z. Tu, W. Tu, Z. Wan, M. Pan, and H. Zhang, *Degradation of silicone rubbers with different hardness in various aqueous solutions*, Polym. Degrad. Stab. 109 (2014), pp. 122–128. doi:10.1016/j.polymdegradstab.2014.07.011
[40] S.Zakaria, P.H.F.Morshuis, M.Y.Benslimane, L.Yu, and A.L.Skov, *The electrical breakdown strength of pre-stretched elastomers, with and without sample volume conservation*, Smart Mater. Struct.24 (2015), pp. 055009. doi:10.1088/0964-1726/24/5/055009